



This document is the accepted manuscript version of a published work that appeared in final form in *Chemical Physics Letters*, © Elsevier, after peer review and technical editing by the publisher. To access the final edited and published work, see <http://dx.doi.org/10.1016/j.cplett.2007.04.018>

(Article begins on next page)

Addressable High-Information-Density DNA Nanostructures

*John Tumpane[‡], Peter Sandin[‡], Ravindra Kumar[†], Vicki E.C. Powers[†], Erik Lundberg[‡], Nittaya Gale[†], Piero Baglioni[#], Jean-Marie Lehn[§], Bo Albinsson[‡], Per Lincoln[‡], L. Marcus Wilhelmsson[‡],
Tom Brown[†], and Bengt Nordén^{†*}*

[‡] Department of Chemical and Biological Engineering / Physical Chemistry, Chalmers University of Technology, SE-41296 Gothenburg, Sweden

[†] School of Chemistry, University of Southampton, Highfield, Southampton SO17 1BJ, UK

[#] Department of Chemistry and CSGI, University of Florence, Dept. Chem., Via Lastruccia 3, Sesto Fiorentino, Florence, I-50019, Italy

[§] Laboratoire de Chimie Supramoléculaire, ISIS, Université Louis Pasteur, 8 allée Gaspard Monge, BP70028, F-67083 Strasbourg Cedex, France

* Telephone: +46-(0)31-7723041

Fax: +46-(0)31-7723858

email: norden@chalmers.se

We present a strategy for self-assembly of the smallest yet reported DNA nanostructures that are also addressable in terms of their DNA-base code. Using linear as well as novel branched three-way DNA oligonucleotide building-blocks we demonstrate the formation of a nano-network's fundamental cell, a DNA pseudo-hexagon of side 4 nm. The network's inherent addressability will allow functionalization with sub-nanometer precision yielding unprecedented richness in information density, important in context of Moore's Law and nano-chip technology.

1. Introduction

An evolution is underway in nanotechnology from top-down (e.g. lithographic) design of nanometer scale structures towards a synthetic, bottom-up strategy based on molecular self-assembly [1]. Among molecules suitable for designing supra-molecular nanometer sized structures DNA is a powerful candidate molecule due to the highly selective hydrogen bonding of the nucleobases and the steric stiffness that their stacking provides to the double-helix structure, along with the ease with which any

Many great endeavors have been made in the field of DNA nanotechnology in recent years, with the complexity of the structures ever-increasing and their size ever-decreasing [2-10]. The pioneering work of Seeman's group has focused mainly upon the use of rigid crossover motifs that reliably build extensive repeating networks which are easily imageable by e.g. AFM, STM [11]. Such crossover motifs are excellent for introducing stability and rigidity to extensive networks but increase significantly the size of the unit-cell by abandoning the simplicity of a single helix. The tetrahedron of Tuberfield and octahedron of Joyce show the possibility to use DNA strands to build approximate geometric shapes and also demonstrate the potential to nano-construct in three dimensions with DNA [12,13]. Nucleic acids with an intrinsic branch-point can be exploited to assemble two and three dimensional structures as demonstrated by the group of von Kiedrowski that has developed branching DNA strands and outlined their obvious applicability to the world of DNA nanotechnology; and more recently the group of Sawai [14-17]. Mimics of the naturally occurring Holliday junctions have also been constructed to demonstrate the appropriateness of distinct branch-points [10]. Aldaye and Sleiman have recently

presented a structure based on rigid linker nodes and 17-mer sides to form a hexameric cyclic construct with a diameter of approximately 15 nm [18].

In order to exploit the inherent advantages afforded by DNA as a bottom-up nanomaterial it is vital to develop non-repetitive networks that are of the smallest possible unit cell size [19]. By using unique, yet short, DNA building-blocks both addressability and unprecedented high information density should be achievable. In both respects we here report a paradigmatic step forward, by constructing DNA pseudo-hexagons, ring-closed structures composed of six sides where each is just one turn (3.4 nm) of duplex DNA, and developed spectroscopic techniques to characterize these structures as well as using the more standard technique of gel electrophoresis to confirm their formation. Novel three-way branched DNA oligonucleotides, have also been developed via a simple and efficient method, based on a new branching monomer compatible with standard automated DNA synthesizers, that allows complete choice of both sequence, directionality and incorporation of modifications for each individual arm. In contrast to all previously reported structures each arm of each three-way node is therefore completely unique. Together with the small unit-size of the network, these properties will allow functionalization with sub-nanometer precision e.g. using triplex-forming oligonucleotides to selectively address a specific position in a network or by direct labeling of the structures. Presented here is a strategy by which oligonucleotides can be assembled into nano-constructs that are the smallest yet reported fundamental cells (<10 nm) of a DNA nano-network and almost half the size of the most recently reported structures(17). Our nanostructures are composed of 10-mer sides, bringing the length down to just one turn of B-DNA, and show the advantage of using semi-flexible linkers (either single-stranded hinges or nodes with semi-flexible side-chains). Using this approach leads to an excellent yield of formation without the need for purification to remove higher-order polymerized structures from the self-assembled mixture. Since a non-integral number of turns introduces strain and the fewer base-pairs involved in holding the structures together would lower the stability, we therefore propose that this is the smallest practically achievable DNA construct that can be made by simple bottom-up self-assembly procedures.

2. Results and discussion

Six 22-mer oligonucleotide strands were designed so as to be complementary to each other in the pattern outlined in Fig. 1a (strands **1-6** = **C**, cyclizable structure). The final ten base-pairs on each end are complementary to a corresponding sequence on one other strand but orthogonal to all other sequences and combinations of such (for more detailed information regarding orthogonal sequence design see Supplementary Information). Two such 10-mer sequences are bridged by two thymines that act as flexible hinges in the constructs. A seventh strand, **5***, was designed for the control construct which is almost identical to the cyclisable one except that one ten base sequence is replaced with all thymines so that ring-closure can not take place in this case, *i.e.* it is a perfect linear analog to our proposed structure (strands **1-4**, **5***, **6** = **L**, linear structure). Submerged gel electrophoresis was performed on these constructs in MetaPhor agarose gel and the results are shown in Fig. 2. (Experimental details for all results are contained in Supplementary Information) The lanes marked **C** contain the constructs that can cyclize, those marked **L** the linear analogue and those marked **C/L** a mixture of both structures. It is clear that the proposed ring structures migrate in a band that is slower than and distinct to that of the uncyclized form. Since the ring-closed form is bulky in two dimensions its rate of migration ought to be slower than that of the linear form to which more pores are accessible and which can wind its way easier through the gel due to a lower friction coefficient. The results indicate that the cyclizable construct is indeed cyclized. The lanes containing both constructs clearly display two bands, corresponding to the individual bands in the other lanes, to verify that they are indeed two unique constructs. More interestingly the lanes carrying the cyclized product contain no significant traces of longer polymerized constructs, nor do they show the presence of any other possible DNA constructs (either shorter or longer). Longer structures would be expected to appear further back in the gel and/or as a streaked band or even trapped at the well. This shows that the structures are formed efficiently (the strands are directly mixed with each other and annealed over 4 hours) and in very high yield, without the need for electrophoretic purification, in stark contrast to the stiffer structures previously reported [18]. This is consistent with intramolecular ring-closure being much more

favourable than intermolecular polymerization confirming that our strategy of using semi-flexible linkers ensures excellent probability of formation. By employing TT hinges we ensure enough flexibility in the system to allow the two ends of a chain to meet without imposing strict geometries via stiff nodes. For this reason the trigonal nodes described later also possess semi-flexible arms to favour nanostructure formation.

UV-melting experiments were then carried out to further characterize the cyclizable system and its linear control (Fig. 3). The derivatives of these plots distinctly show a characteristic difference. The pseudo-hexagonal construct shows a very steep and sharp peak upon initial melting at 31°C that is absent for its non-cyclized counterpart. This represents the thermodynamic strain inherent to the ring-closed system due to a significant “immobilization entropy”. It also implies that ring-opening is a very co-operative and instantaneous process which is what one would expect from such an event. Once this strain is released the two curves are essentially identical suggesting that the processes that are then occurring are, as expected, very similar in nature.

Since we are now working at a scale below what is typically probed via AFM for DNA studies it was deemed necessary to complement the electrophoretic evidence with the development of spectroscopic techniques which are more appropriate at this scale. Fluorescence resonance energy transfer (FRET) measurements were therefore carried out on these systems which were strategically labeled with the donor chromophore, fluorescein - attached to strand **1** at the 5'-terminus and the acceptor chromophore, Cy3 - labeled on the 5'-terminus of one of the other strands (**2-6, 5***) for all possible combinations (See Fig. 1). The energy transfer efficiencies for each differently labeled construct are shown in Fig. 3. For the cyclized structure **C6**, where the acceptor chromophore is attached to oligonucleotide **6**, the formation of a ring will position the acceptor chromophore a distance of only one DNA turn (3.4 nm) and two hinges away from the donor chromophore which should lead to high energy transfer efficiency. By contrast, for the linear structure **L6**, as a consequence of a large separation of acceptor and donor chromophores, there should be negligible or no detectable energy transfer. Indeed, this is what we find when comparing the energy transfer measured for the **C6** (66 %) and **L6** assembly (5 %). High

efficiency of energy transfer in the C assembly would also be expected if the six oligonucleotides were to form a longer linear polymer but as seen in the electrophoretic measurements this possibility has already been ruled out. The energy transfer when modifying the acceptor position in the C assembly decreases in the order: **C2>C6>C3>C5>C4**. Despite the dynamics of the construct, including the flexibility of the fluorophore linkers and the rotational freedom of each of the DNA duplexes, this trend is in exact qualitative agreement with that expected from the schematic in Fig. 1a. As for the linear assemblies, the energy transfer efficiencies for **L4**, **L3** and **L2** are 13, 28 and 76 %, respectively (the donor and acceptor of **L6** and **L5*** are too far apart for significant energy transfer). The distances in the linear assemblies should increase in the order: **L2<L3<L4<L5*<L6** which is in perfect agreement with the FRET results, thus, further justifying the application of FRET to deduce the closed structure and to confirm that it is of the size expected by ring-closure of this six-sided object to form a pseudo-hexagon. Importantly, these measurements also show that it is possible to achieve relatively high energy transfer efficiencies in such a system, something that is impossible with larger unit-cell sizes since FRET efficiency decreases with the sixth power of distance and is not usually detectable beyond 10 nm. Thus, not only have we established that FRET is an excellent technique for characterization of ultra-small nano-networks but also that the transmission of energy is possible within such networks.

With the aim of building extended non-repetitive networks in mind we developed unique three-way DNA nodes based on both symmetric and asymmetric monomers branching phosphoramidite monomers (See Supplementary Information and Brown, T. et al, manuscript in preparation). These nodes each have three unique arms which means they are the essential element of a non-repeating addressable network. Because of the desire to keep the node small and to have a symmetric geometry about the nodal point, a monomer based on a 1,3,5-tri-substituted benzene ring was chosen, as shown in Fig. 4. The use of orthogonal protecting groups ensures that, unlike previously reported branching monomers, three entirely different oligonucleotide sequences can be situated on the same trigonal node by solid-phase synthesis and that there is full freedom of choice in directionality (*i.e.* 5'-3' or 3'-5') and functionalization for each arm. In the examples given here the direction of one arm is 3'-5' and the

other two are 5'-3'. Other nodes have been synthesized in which all arms are 5'-3' or all 3'-5'. This is achieved by the appropriate use of reverse phosphoramidite monomers (Link Technologies Ltd). Using the symmetrical node monomer it is possible to ensure geometric symmetry whilst having full sequence asymmetry at the branch points, this being an integral part of the strategy to develop addressable nanostructures. Furthermore this novel monomer is, importantly, perfectly compatible with the automated solid-phase synthesis process. In order to directly compare structures formed by these new oligonucleotides with those already characterized and self-assembled from standard DNA strands, six three-way oligonucleotides (1^T-6^T) were synthesized where two of the arms on each node are the same sequences as the orthogonal ones used in the structures outlined above and the third arm on each is a unique orthogonal sequence to those already used and all other new arms (See Supplementary Information for full design). Again a seventh oligonucleotide was synthesized (5^{*T}) that would act as a reference non-cyclizable construct. The structures are indicated in Fig.4, where the same color-coding as in Fig. 1 is employed. The complementary strands to the six protruding arms were synthesized as standard 10-mers oligos so that each structure is constructed from a total of 12 strands to form an entirely double-stranded nanostructure. In order to confirm ring-closure the structures were directly compared in a gel electrophoresis experiment similar to the one performed on the standard oligo analogs. One of the three-way oligonucleotides, 6^T , was labeled with Cy3 which was used to image the structures in the gel. Again we see a distinct difference in mobility for the two constructs, the cyclized form migrating more slowly than the non-cyclizable form. The same reasoning can be used here to explain the difference in mobilities as for the standard DNA constructs although the resolution between the two structures is even better here. The protruding arms of the trigonal node constructs must have an “anchoring effect” in the pores where they increase friction which then further reduces the mobility of the cyclized form. Furthermore, there is obviously also a very high yield of formation for the cyclized construct proving that this linker node is still flexible enough to allow ring-closure and thus nanostructure formation whilst still imposing the correct geometry. Further details on yield of formation can be found in the Supplementary Material. As a non-trivial proof of principle for addressability an

electrophoresis experiment was devised where three of these pseudo-hexagonal constructs were formed and a different side-arm of each construct selectively addressed using an oligonucleotide labeled at the 5' terminus with Cy3. The gel shows that in each case the bands have the same mobility as detected by the fluorescence from Cy3. Any difference in fluorescence intensity can be attributable to the change in quantum yield for Cy3 which is sequence dependent or small differences in sample volume when loading the wells. One must therefore conclude that we have constructed the same pseudo-hexagonal construct in each case but that the Cy3 label occupies a different position in what are otherwise identical nanostructures

3. Conclusions

The efficient self-assembly and verification of formation of a hexagonal DNA nano-network unit cell, which is the smallest yet reported, are important steps forward in nano-network research. The complete freedom of sequences and functionalization of normal as well as trigonal DNA, provides a basis for selectively addressing a specific position of a network using, as demonstrated here, a Cy3 fluorophore or for example triplex-forming oligonucleotides [20,21]. The small cell size (<10 nm) of this pseudo-hexagon, an order of magnitude smaller than previous repeating DNA networks, demands a different approach to structural characterization. With decreasing cell size conventional techniques, such as microscopy, for studying DNA nano-networks become increasingly difficult and spectroscopic methods are instead required. In particular, FRET works excellently in the 1–10 nm range. Here the combined results from FRET, UV-melting and gel electrophoresis establish the exclusive formation of a pseudo-hexagonal nano-network unit cell with only one B-DNA duplex turn (3.4 nm) per side. A shorter duplex would have too low a melting temperature and would also be likely to introduce excess tension to the hexagon due to incomplete helix-turns. Thus, we claim our orthogonal DNA nano-network cell to be the smallest achievable. Potential applications of this type of high-density nano-network include information storage and transfer. The FRET results demonstrate that this cell size allows controlled transfer of energy through predetermined paths in such a DNA network.

Acknowledgments

We thank Professor Björn Åkerman for discussions and advice regarding gel electrophoresis. This research is funded by the European Commission's Sixth Framework Programme (Project reference AMNA, contract no. 013575)

Supplementary Information

Design of sequences used, experimental details and synthesis of three-way nodes/oligonucleotides.

References

- [1] G. M. Whitesides, J. C. Love, *Sci. Am.* 285 (2001) 38.
- [2] J. Qi, X. J. Li, X. P. Yang, N. C. Seeman, *J. Am. Chem. Soc.* 118 (1996) 6121.
- [3] S. H. Park, C. Pistol, S. J. Ahn, J. H. Reif, A. R. Lebeck, C. Dwyer, T. H. LaBean, *Angew. Chem.-Int. Edit.* 45 (2006) 735.
- [4] B. Q. Ding, R. J. Sha, N. C. Seeman, *J. Am. Chem. Soc.* 126 (2004) 10230.
- [5] Y. He, Y. Chen, H. P. Liu, A. E. Ribbe, C. D. Mao, *J. Am. Chem. Soc.* 127 (2005) 12202.
- [6] T. H. LaBean, H. Yan, J. Kopatsch, F. R. Liu, E. Winfree, J. H. Reif, N. C. Seeman, *J. Am. Chem. Soc.* 122 (2000) 1848.
- [7] F. Mathieu, S. P. Liao, J. Kopatsch, T. Wang, C. D. Mao, N. C. Seeman, *Nano Lett.* 5 (2005) 661.
- [8] N. C. Seeman, *Nano Lett.* 1 (2001) 22.
- [9] W. B. Sherman, N. C. Seeman, *Nano Lett.* 4 (2004) 1203.
- [10] N. C. Seeman, P. S. Lukeman, *Rep. Prog. Phys.* 68 (2005) 237.
- [11] N. C. Seeman, *Nature* 421 (2003) 427.
- [12] W. M. Shih, J. D. Quispe, G. F. Joyce, 427 (2004) 618.
- [13] R. P. Goodman, I. A. T. Schaap, C. F. Tardin, C. M. Erben, R. M. Berry, C. F. Schmidt, A. J. Turberfield, *Science* 310 (2005) 1661.
- [14] G. von Kiedrowski, L. H. Eckardt, K. Naumann, W. M. Pankau, M. Reimold, M. Rein, 75 (2003) 609.
- [15] L. H. Eckardt, K. Naumann, W. M. Pankau, M. Rein, M. Schweitzer, N. Windhab, G. von Kiedrowski, *Nature* 420 (2002) 286.
- [16] M. Scheffler, A. Dorenbeck, S. Jordan, M. Wustefeld, G. von Kiedrowski, *Angew. Chem.-Int. Edit.* 38 (1999) 3312.
- [17] T. Kuroda, Y. Sakurai, Y. Suzuki, A. O. Nakamura, M. Kuwahara, H. Ozaki, H. Sawai, 1 (2006) 575.
- [18] F. A. Aldaye, H. F. Sleiman, *Angew. Chem.-Int. Edit.* 45 (2006) 2204.
- [19] CORDIS, EU Nanotechnology Research: Exploring the Fundamentals, 2005.
- [20] D. A. Rusling, V. E. C. Powers, R. T. Ranasinghe, Y. Wang, S. D. Osborne, T. Brown, K. R. Fox, *Nucleic Acids Res.* 33 (2005) 3025.
- [21] K. R. Fox, *Curr. Med. Chem.* 7 (2000) 17.

Figure 1. Design of nano-sized DNA pseudo-hexagons and evidence of formation by gel electrophoresis

(a) A color-coded schematic showing the orthogonal design of the oligonucleotides for the cyclizable construct, C, and the non-cyclizable linear analog, L. Sequences are numbered at their 5'-termini with arrowheads representing the 3'-terminus. TT hinges are indicated in black. The C assembly consists of six 22-mer oligonucleotide sequences (**1–6**) designed to hybridize to each other to form a pseudo-hexagon. The 22-mers are designed to have two different 10-mer outer regions complementary to a corresponding region on two other 22-mers and orthogonal (≤ 4 consecutive matching bases) to any other part of all the sequences (see Supplementary Information). The L assembly consists of five of the six oligonucleotide sequences of the C assembly (**1–4** and **6**) and an additional 22-mer sequence, **5***, designed to also be orthogonal to **2**, thus, preventing ring closure of the oligonucleotides. Three-dimensional schematic representations are also shown.

(b) Gel electrophoresis experiments performed in 4.5% MetaPhor agarose. Lanes containing only cyclisable nanostructures are marked by C, only non-cyclizable by L or a mixture of the two by C/L. Gels were run at 4.5 V cm^{-1} , 4° C and post-stained with ethidium bromide. Total concentration of hexagon or linear form is $0.33 \text{ }\mu\text{M}$. Measurements performed at 7° C using a phosphate buffer (pH 7.5, total Na^+ concentration is 200 mM).

Figure 2. UV-melting experiments

UV melting temperature experiments were performed on the C (black line) and L assemblies (red line) shown in Fig. 1. Inset shows first derivative of unnormalized melting curves of the C (black line) and L assemblies (red line). Ring-opening occurs at 31° C

Figure 3. Fluorescence resonance energy transfer: evidence of ring-closure of DNA nano-constructs

Comparison of energy transfer efficiency in cyclized (black bars) and corresponding linear (red bars) nano-sized DNA constructs. The cyclized, C, and the linear form, L, have a fluorescein donor label attached to the 5'-terminus of oligonucleotide **1**. In the comparisons C/L6, C5/L5*, C/L4, C/L3 and C/L2, sequence **6**, **5** or **5***, **4**, **3**, and **2**, respectively, have a Cy3 acceptor label attached to the 5'-terminus.

Figure 4. Trigonal DNA monomer and its use in building addressable DNA nano-constructs

(a) Schematic showing the three-way oligonucleotides used to build the structures, the color-coding shows their complementarity as well as how they compare to the structures made from standard oligonucleotides (See Fig.1). Standard 10-mer oligos were used as complements to the protruding arms.

(b) Symmetric three-way node, based a 1,3,5-trisubstituted benzene with three orthogonal protecting groups. This monomer is perfectly compatible with automated oligonucleotide synthesis.

(c) Gel electrophoresis of the cyclized C^T and linear L^T assemblies built from these three-way nodes. The lane marked C^T contains only the cyclisable structures, L^T only the linear structure. Electrophoretic conditions are as described in Fig. 1.

(d) The same construct, C^T selectively addressed at three individual sites with a Cy3 fluorophore. The superscript indicates the node which was addressably targeted by the Cy3 labeled 10-mer. L^{T4} was the corresponding linear reference construct and N⁴ a single node with one Cy3 labeled complementary strand. Since all constructs have the same mobility the pseudo-hexagonal construct must be successfully addressed in these three different positions.

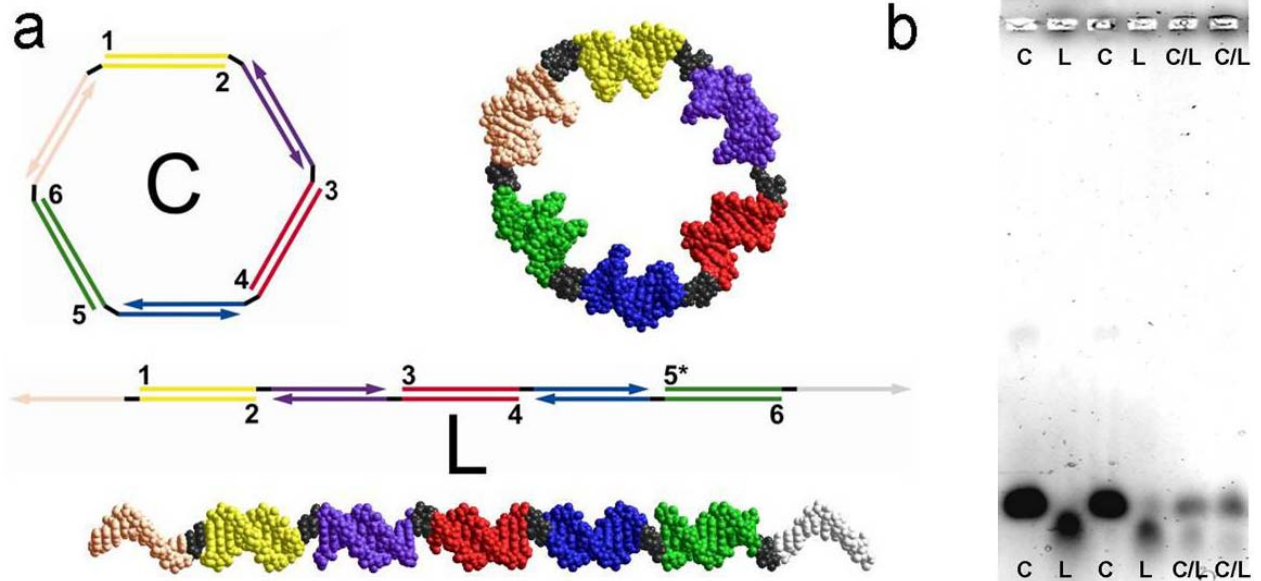


Figure 1

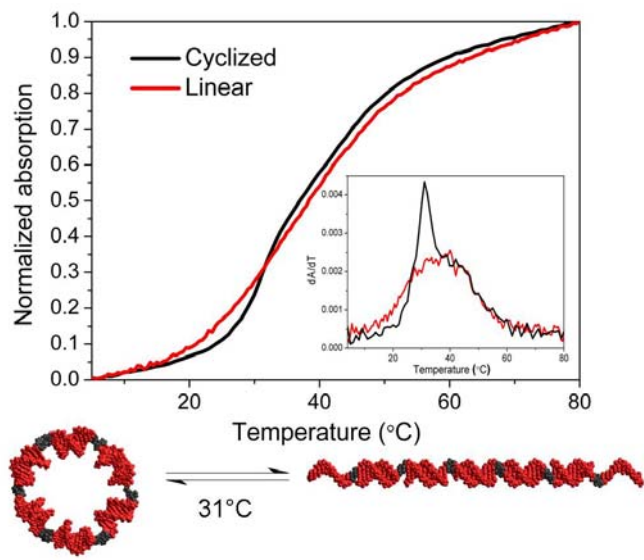


Figure 2

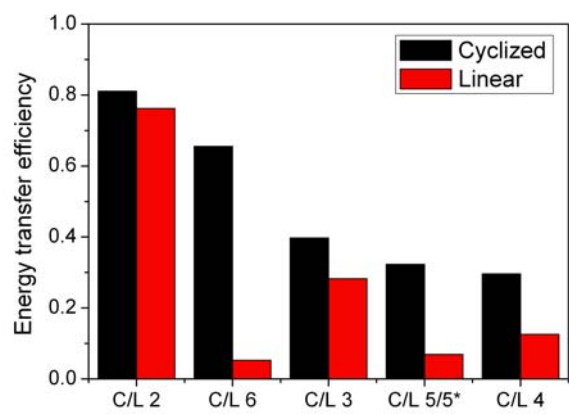


Figure 3

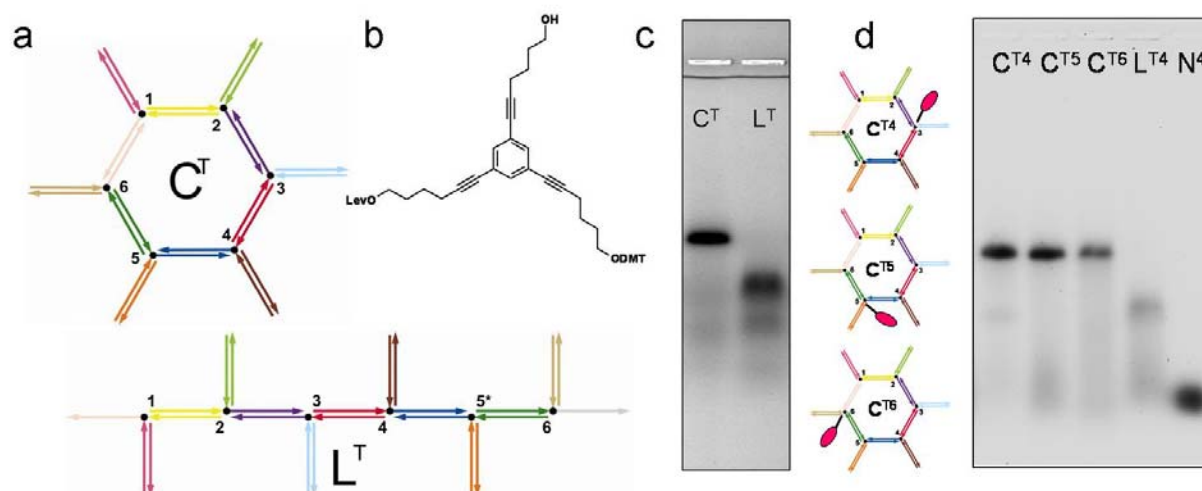


Figure 4